Driving Force of Stacking-Fault Formation in SiC *p-i-n* Diodes

S. Ha and M. Skowronski

Department of Materials Science and Engineering, Carnegie Mellon University, 5000 Forbes Avenue, Pittsburgh, Pennsylvania 15213, USA

J. J. Sumakeris, M. J. Paisley, and M. K. Das

Cree, Inc., 4600 Silicon Drive, Durham, North Carolina 27703, USA

(Received 24 November 2003; published 30 April 2004)

The driving force of stacking-fault expansion in SiC *p-i-n* diodes was investigated using optical emission microscopy and transmission electron microscopy. The stacking-fault expansion and properties of the partial dislocations were inconsistent with any stress as the driving force. A thermodynamic free energy difference between the perfect and a faulted structure is suggested as a plausible driving force in the tested diodes, indicating that hexagonal polytypes of silicon carbide are metastable at room temperature.

DOI: 10.1103/PhysRevLett.92.175504 PACS numbers: 61.72.Ff, 81.05.Hd, 85.30.Kk

Silicon carbide (SiC) is a promising wide band gap semiconductor suited for numerous applications such as high speed communications, high efficiency electric power control systems, and sensors operating in hostile environments [1]. In contrast to other wide band gap semiconductors such as diamond and group III nitrides, hexagonal SiC polytypes are available in large single crystal wafer form [2], which has accelerated the development and commercialization of high voltage and high frequency electronic devices [2,3]. However, recent reports on the degradation of the forward characteristics of SiC *p-i-n* diodes brought up questions about the stability of this material [4]. Several studies revealed that the phenomenon occurs both in 4H-SiC and 6H-SiC and is due to the formation of Shockley-type stacking faults in the diode structure [5–13]. Since such stacking faults are known to form by shear, stress in the diode structure has been proposed as the driving force of their formation and expansion [6,10,11]. In this study, we tested this hypothesis by comparing the motion and properties of partial dislocations bounding the stacking faults. The results indicate that, in addition to the mechanical stress which can drive the stacking-fault expansion in diodes with a significant level of stress, there is an additional mechanism causing this phenomenon in diodes with low stress.

The *p-i-n* diodes examined in this study were fabricated on 3 in. diameter, 4H-SiC, *n*-type ($n \sim 8 \times 10^{18}$ cm^{-3}) substrates. The substrates were off cut by 8° from the [0001] toward a [11-20] direction and the diodes were fabricated on the silicon-terminated surface. The low-doped blocking layer (n or $p \sim 10^{14}$–10^{15} cm^{-3}) and the *p*-type anode ($p \sim 10^{18}$ cm^{-3}) were deposited by chemical vapor deposition. Standard metal contacts were formed on the anode surface and substrate backside. Diode mesas were defined by reactive ion etching. The detailed design and fabrication procedures of the diodes have been described elsewhere [14]. The evolution of dislocations in SiC layers was recorded employing optical emission microscopy (OEM). For this, the top contact layer of the diodes was formed in a grid pattern with windows making it possible to observe dislocations by electroluminescence. The OEM equipment consisted of a liquid-nitrogen cooled (− 100 °C), UV sensitive charge-coupled device (CCD) camera and an optical microscope mounted on a probe station. The OEM images were collected under forward bias with the current density of 1.0 A/cm^2. Typical exposure time was approximately 1 min. Under such conditions, most dislocations remained stationary with some exceptions traveled by a maximum distance of 10 μm.

Several diodes were selected for transmission electron microscopy (TEM) analysis of the partial dislocations bounding the stacking faults. Their Burgers vectors and line directions were determined applying an oscillating contrast analysis proposed by Marukawa [15]. The detailed sample preparation and analysis methods have been described elsewhere [13]. The TEM observations were performed on a Philips EM420 microscope operated at 120 kV.

During the OEM experiments, movement of partial dislocations and formation of stacking faults were observed in both diode structures with either an *n*-type or a *p*-type blocking layer. Figure 1 shows plan-view OEM images of a part of a diode taken at different stages of degradation under forward bias. The black grid lines are the top metal contacts and the small square-shaped gray areas correspond to SiC seen through the metallization windows. Figure 1(a) is the image of a "virgin" diode. Numerous bright spots and a few short line segments are visible within the windows corresponding to dislocations in the blocking layer. Since the image is a top view, the bright lines correspond to basal plane dislocations while the bright dots are threading dislocations with

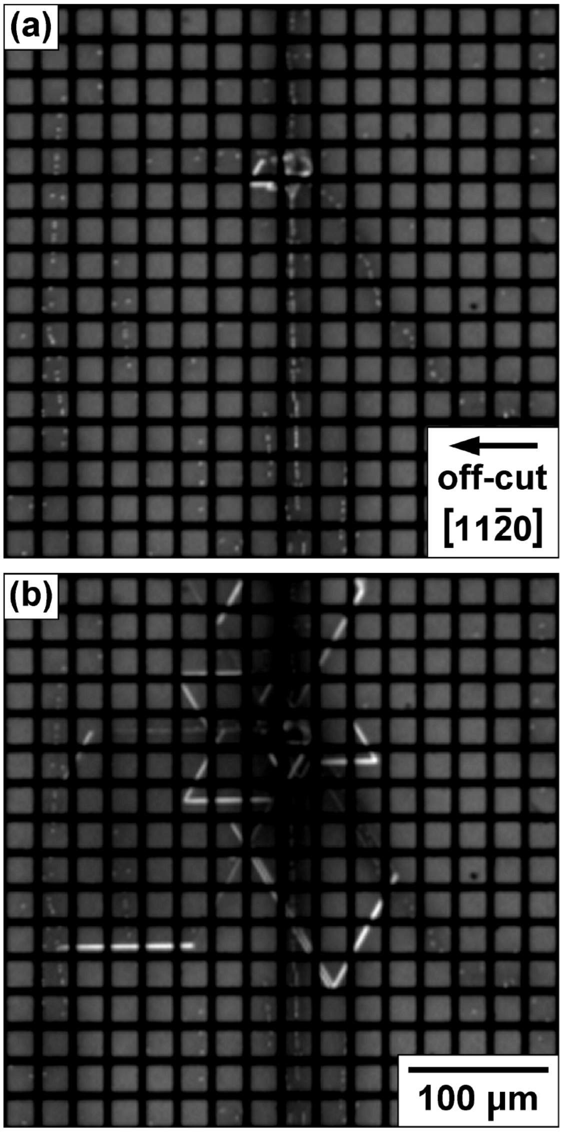

FIG. 1. Plan-view optical emission microscopy images showing a simultaneous development of various rhombic stacking faults in a 4H-SiC *p-i-n* diode: (a) the "virgin" diode before degradation showing the preexistent dislocations in the blocking layer. The 8° offcut toward the [11-20] direction is marked with an arrow; (b) the same area after 5 min of biasing at 50 A/cm^2. Numerous wedge-shaped bright lines emanated from a point source corresponding to rhomb-shaped Shockley-type stacking faults in basal planes.

line directions close to the surface normal. The light emission is due to electrons and holes recombining preferentially along dislocation lines. Of particular interest is the cluster of bright lines and spots located above the center of the image. Figure 1(b) shows the same location after 5 min of high current biasing at 50 A/cm^2. A number of new wedge-shaped bright lines appeared around the cluster which apparently served as a nucleation source of dislocations. Each wedge and the center of the cluster together form a rhombus. During the high current biasing, the bright wedges emanated from the center and moved in the direction of the long diagonal of each rhombus. TEM [6,11,13] and x-ray topography [5,8,9] studies have identified the rhombic areas swept by the wedges as single-layer Shockley-type stacking faults in basal planes of 4H-SiC. The stacking-fault expansion continued with prolonged biasing until bright lines reached a boundary such as the diode edges, the top surface, or the interface between the blocking layer and the substrate. Such simultaneous nucleation of several rhombic stacking faults from a point source was observed several times in diodes fabricated on different wafers.

Shockley-type stacking faults are created as the consequence of glide of partial dislocations and are bounded by them. Rhombic stacking faults in SiC *p-i-n* diodes originate from point-shaped sources and are bounded by partial dislocation loops with a single Burgers vector (**b**) parallel to the long diagonal of the rhombus [9]. The partial dislocations are aligned along the ⟨11-20⟩ directions as seen in Fig. 1(b), which correspond to the locations of Peierls valleys in hexagonal SiC polytypes. Only two of the four dislocation segments surrounding a rhombus move and emit bright visible light during biasing. The other two sides remain stationary and exhibit very weak emission in the detection range of the silicon-based CCD camera. We have recently determined that the mobile dislocation segments have cores consisting of only silicon atoms [13]. Such a partial dislocation is denoted as Si(g) and the extra plane of atoms associated with its edge component is positioned from the dislocation line toward the silicon-terminated surface of the crystal. From the above results, one can determine the Burgers vector direction of a rhombic dislocation loop: it is parallel to the long diagonal of the rhombus and points toward the apex formed by two Si(g) partial dislocation segments. The same Burgers vector was observed in the present TEM analysis of the partial dislocations. In this assignment, the line sense (**u**) of the dislocation loop is chosen to be in the clockwise direction while the silicon-terminated surface faces the reader. Throughout this paper, a Burgers vector is defined following the convention used by Hirth and Lothe [16].

Either local or uniform stress in the diode structure has been proposed by several groups as the driving force of the stacking-fault formation [6,10,11]. Typically, a dislocation glides in its glide plane in response to a resolved shear stress (**t**) in that plane. Depending on the dot product $\mathbf{b} \cdot \mathbf{t}$, a dislocation moves in one direction or the other. Thus, knowing the glide direction and the Burgers vector of a dislocation, one can deduce the sign of shear stress. Accordingly, we have analyzed the stacking faults and their bounding partial dislocations and determined the shear stress driving their motion. Figure 2 illustrates the analysis of Fig. 1 as an example and shows six rhombic dislocation loops (a)–(f) that can form in the diodes. The solid lines represent mobile, luminescent segments, while

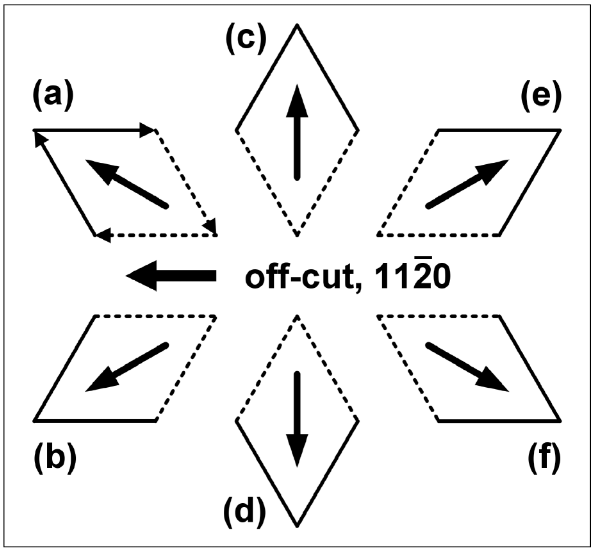

FIG. 2. Schematic analysis of Fig. 1. Each rhombus is a Shockley-type stacking fault bounded by a partial dislocation loop. The loops consist of solid and broken lines corresponding to luminescent, mobile and dark, stationary segments, respectively. The partial dislocation segments are all aligned along the Peierls valleys, the ⟨11-20⟩ directions. The arrow in each rhombus is the Burgers vector of the bounding partial dislocation loop.

the broken lines stationary, dark segments. The arrow inside each rhombus designates its Burgers vector direction. The Burgers vector and line sense are assigned following the convention described above. This is shown in (*a*) as an example. The extra plane of atoms is toward the positive direction of the vector product $\mathbf{u} \times \mathbf{b}$. One can see that the vector product points toward the reader for the solid lines [Si(*g*)] and away from the reader for the broken lines [C(*g*)]. Each loop will expand or contract independently in response to a shear stress. If the dot product of the Burgers vector and the shear stress acting on the reader's side of the glide plane (plane of figure) is positive, the loop will expand. One can see in Fig. 2 that no single stress in one direction can drive all six loops to expand simultaneously. However, it is clearly seen in Fig. 1 that five different rhombic stacking faults grew at the same time. This is direct evidence of the fact that the stacking-fault expansion occurring in the tested diodes was not due to a uniform long range stress in the blocking layer.

One may argue that there can be a point source of local stress around which the stress direction changes to develop different stacking faults as in Fig. 1. In that case, the stress level has to decrease with the distance from the source and the stacking-fault growth should gradually slow down and eventually stop. In our experiments, the different rhombic stacking faults grew to the limit of the diode area (1.2×1.2 mm^2) which is beyond the scale of a local stress.

A similar conclusion can be reached by the analysis of another example (Fig. 3). The OEM images were taken in a series from the same area of another diode. The diode was biased at the current density of 50 A/cm^2 for 1 min between the exposures. In Fig. 3(a), there are two wedge-shaped bright lines in the top left and bottom right regions, which are the mobile front segments of two rhombic stacking faults. Their Burgers vectors are opposite to each other according to our convention. The top one expanded downward during the biasing while the other upward as seen in Figs. 3(b) and 3(c). Such simultaneous motions cannot be explained by one uniform stress as discussed in Fig. 2. It is possible, however, that their expansions had been due to two different sources of local stress, producing opposite resolved shear stress components parallel to the Burgers vector. In such a case, the opposite components should cancel each other in the area where the partial dislocations approach each other. As a result, their motion should cease before cross-over. However, they passed each other and continued expansion as shown in Fig. 3(c). The above observations point out that the major driving force of the stacking-fault growth in the tested 4H-SiC *p-i-n* diodes is not mechanical stress, neither local nor long range. It should be pointed out that the Shockley-type stacking faults should form preferentially in one direction if the stress in the diodes exceeds a certain level. Our observations indicate that there was no significant stress in the tested diode structure.

Lindefelt *et al.* [17] and Miao *et al.* [18] performed first principle calculations of the electronic structure and energy of the single-layer Shockley-type stacking fault in 4H-SiC. Both groups concluded that the stacking fault results in a quantum-well-like defect state in the band gap with a depth of 0.2–0.3 eV below the conduction band, and that the stacking-fault energy is of the order of a few

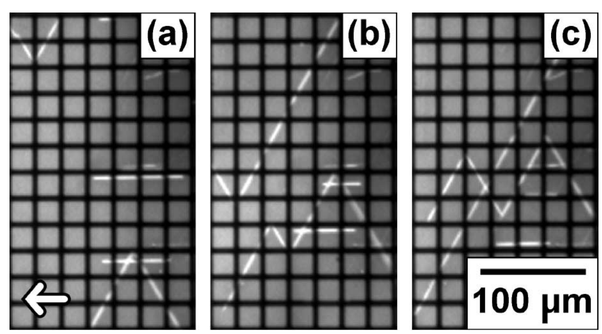

FIG. 3. Plan-view optical emission microscopy images showing the development of two rhombic stacking faults. The diode was biased between exposures at the current density of 50 A/cm^2 for 1 min: (a) Two wedge-shaped Si(*g*) mobile fronts of the rhombic stacking faults are in the top left and bottom right regions. The 8° offcut toward the [11-20] direction is marked with an arrow; (b),(c) the two bright wedges moved in opposite directions and passed each other.

meV per atomic pair. Comparing these energies, Miao *et al.* further suggested that reduction of conduction electron energy associated with the stacking-fault state would favor the formation of stacking faults in n-type material. However, the formation of stacking faults in the diodes cannot be caused by this electronic effect since we have observed it to occur in p-type material.

Considering all the above arguments, we suggest the thermodynamic free energy difference between different stacking sequences of SiC as the next plausible driving force for the stacking-fault formation. In other words, hexagonal polytypes of SiC are metastable at room temperature and would convert to a faulted structure if the activation energy for the partial dislocation glide is available. This activation energy is provided by the electron-hole recombination during operation of the diodes [9,18–20]. Limpijumnong and Lambrecht [21] have predicted that 4H, 6H, and 15R polytypes are more stable than 3C. The energy differences between them, however, are very small and it is conceivable that the sequence could be reversed at least in certain conditions.

This work was supported in part by ONR Contract No. N00014-02-C-0302 monitored by Dr. Harry Dietrich.

[1] M. A. Capano and R. J. Trew, Mater. Res. Bull. **22**, No. 3, 19 (1997).
[2] St. G. Müller, M. F. Brady, W. H. Brixius, R. C. Glass, H. McD. Hobgood, J. R. Jenny, R. T. Leonard, D. P. Malta, A. R. Powell, V. F. Tsvetkov, S. T. Allen, J.W. Palmour, and C. H. Carter, Jr., Mater. Sci. Forum **433–436**, 39 (2003).
[3] R. Rupp and I. Zverev, Mater. Sci. Forum **433–436**, 805 (2003).
[4] H. Lendenmann, F. Dahlquist, N. Johansson, R. Söderholm, P. A. Nilsson, J. P. Bergman, and P. Skytt, Mater. Sci. Forum **353–356**, 727 (2001).
[5] J. P. Bergman, H. Lendenmann, P. Å. Nilsson, and P. Skytt, Mater. Sci. Forum **353–356**, 299 (2001).
[6] J. Q. Liu, M. Skowronski, C. Hallin, R. Söderholm, and H. Lendenmann, Appl. Phys. Lett. **80**, 749 (2002).
[7] R. E. Stahlbush, M. Fatemi, J. B. Fedison, S. D. Arthur, L. B. Rowland, and S. Wang, J. Electron. Mater. **31**, 827 (2002).
[8] H. Jacobson, J. Birch, R. Yakimova, M. Syväjärvi, J. P. Bergman, A. Ellison, T. Tuomi, and E. Janzén, J. Appl. Phys. **91**, 6354 (2002).
[9] M. Skowronski, J. Q. Liu, W. M. Vetter, M. Dudley, C. Hallin, and H. Lendenmann, J. Appl. Phys. **92**, 4699 (2002).
[10] P. O. Å. Persson, L. Hultman, H. Jacobson, J. P. Bergman, E. Janzén, J. M. Molina-Aldareguia, W. J. Clegg, and T. Tuomi, Appl. Phys. Lett. **80**, 4852 (2002).
[11] M. E. Twigg, R. E. Stahlbush, M. Fatemi, S. D. Arthur, J. B. Fedison, J. B. Tucker, and S. Wang, Appl. Phys. Lett. **82**, 2410 (2003).
[12] M. Zhang, P. Pirouz, and H. Lendenmann, Appl. Phys. Lett. **83**, 3320 (2003).
[13] S. Ha, M. Benamara, M. Skowronski, and H. Lendenmann, Appl. Phys. Lett. **83**, 4957 (2003).
[14] R. Singh, K. G. Irvine, D. C. Capell, J. T. Richmond, D. Berning, A. R. Hefner, and J.W. Palmour, IEEE Trans. Electron Devices **49**, 2308 (2002).
[15] K. Marukawa, Philos. Mag. A **40**, 303 (1979).
[16] J. P. Hirth and J. Lothe, *Theory of Dislocations* (Krieger Publishing Company, Malabar, 1982), 2nd ed., pp. 17–24.
[17] U. Lindefelt, H. Iwata, S. Öberg, and P. R. Briddon, Phys. Rev. B **67**, 155204 (2003).
[18] M. S. Miao, S. Limpijumnong, and W. R. L. Lambrecht, Appl. Phys. Lett. **79**, 4360 (2001).
[19] A. Galeckas, J. Linnros, and P. Pirouz, Appl. Phys. Lett. **81**, 883 (2002).
[20] J. P. Bergman, H. Jakobsson, L. Storasta, F. H. C. Carlsson, B. Magnusson, S. Sridhara, G. Pozina, H. Lendenmann, and E. Janzén, Mater. Sci. Forum **389–393**, 9 (2002).
[21] S. Limpijumnong and W. R. L. Lambrecht, Phys. Rev. B **57**, 12 017 (1998).